ELSEVIER

Comminution and fluidization of granular fault materials: implications for fault slip behavior

Nobuaki Monzawa[1], Kenshiro Otsuki*

Department of Geoenvironmental Sciences, Graduate School of Science, Tohoku University, Aobayama, Aoba, Sendai 980-8578, Japan

Abstract

Whilst faulting in the shallow crust is inevitably associated with comminution of rocks, the mechanical properties of the comminuted granular materials themselves affect the slip behavior of faults. Therefore, the mechanical behavior of any fault progresses along an evolutionary path. We analyzed granular fault rocks from four faults, and deduced an evolutionary trend of fractal size frequency. Comminution of fault rocks starts at a fractal dimension close to 1.5 (2-D measurement), at which a given grain is supported by the maximum number of grains attainable and hence is at its strongest. As comminution proceeds, the fractal dimension increases, and hence comminution itself is a slip weakening mechanism. Under the appropriate conditions, comminuted granular materials may be fluidized during seismic slip events. In this paper, we develop a new method to identify the granular fault rocks that have experienced fluidization, where the detection probability of fragmented counterparts is a key parameter. This method was applied to four fault rock samples and a successful result was obtained. Knowledge from powder technology teaches us that the volume fraction of grains normalized by maximum volume fraction attainable is the most important parameter for dynamic properties of granular materials, and once granular fault materials are fluidized, the fault plane becomes nearly frictionless. A small decrease in the normalized volume fraction of grains from 1 is a necessary condition for the phase transition to fluidization from the deformation mechanism governed by grain friction and crushing by contact stresses. This condition can be realized only when shearing proceeds under unconstrained conditions, and this demands that the gap between fault walls is widened. Normal interface vibration proposed by Brune et al. [Tectonophysics 218 (1993) 59] appears to be the most appropriate cause of this, and we presented two lines of field evidence that support this mechanism to work in nature.
© 2003 Elsevier Science B.V. All rights reserved.

Keywords: Fault gouge; Cataclasite; Comminution; Grain size frequency; Fluidization; Normal interface vibration

1. Introduction

Faulting in the brittle field is characterized by comminution of rocks, yet inversely the mechanical properties of comminuted granular materials (fault gouge and cataclasite) themselves strongly affect fault slip behavior. This interactive relationship between faulting and fault materials is very complex, and many geologists and geophysicists have approached to this problem from diverse viewpoints:

1. Comminution is a process in which a part of the released elastic stain energy is dissipated as surface

---

* Corresponding author. Tel.: +81-22-217-6614; fax: +81-22-217-6634.

E-mail address: otsuki@dges.tohoku.ac.jp (K. Otsuki).

[1] Now in Japan Energy Development Co., LTD., 1F, Sankaido Building, 9-13, Akasaka 1-chome, Minato, Tokyo 107-0052, Japan.

energy, and it is related to seismic efficiency. The grain size frequency, necessary to estimate surface energy, has been measured for natural and experimental gouges and cataclastic rocks. Most granular fault rocks show a fractal nature and the physical meaning of this has been discussed. The surface energy is proportional to the total area of grains surfaces, which is estimated by integrating for surface density over the zone of comminution. Many data show a proportional relationship between fault width and total displacement of a fault, but comminution is sometimes concentrated into very thin zones (fault core).

2. Faulting and rock comminution are considered as a kind of dissipative process, and hence are inevitably associated with a characteristic pattern of deformation within the comminution zone. Shear strain in the case of stable sliding tends to be accommodated by homogeneous cataclasis over the shear zone, while in the case of stick–slip it tends to be localized to narrow slip zones like Riedel shear. The geometry of the structures inside comminution zones is believed to be a rich source of information on the fault dynamics.

3. Mechanical properties of fault rocks govern the slip behavior of faults, and they are of course dependent on material types, temperature, pressure, imposed strain rate and chemical reactions. When comminuted fault materials can be modeled as granular materials, stain is accommodated by two kinds of microscopic processes; frictional sliding and crushing of closely packed grains under constrained conditions, and fluidization in which loosely packed grains are allowed to move with a mean free path.

In the first part of this paper we focus on the evolutionary trend of comminution of fault rocks in conjunction with the first issue above, and the weakening process of granular materials will be discussed in relation to the evolution grain packing. Fluidization of granular fault materials, which is a part of the third issue above, has a significant effect on seismic frictional resistance on fault planes. We will present a new method for identifying the granular fault rocks that have experienced fluidization, and the analytical result for natural fault rocks also is shown. Frictional properties of fluidized granular materials, which have been studied intensively in powder technology, are reviewed and their effect on seismic slip behavior is discussed. Finally, two lines of field evidence that support the normal interface vibration, the most plausible cause of fluidization, will be presented.

2. General description of granular fault rock samples and their geologic setting

The fault rock samples dealt with in this paper were collected from four faults in Japan: the Tanakura shear zone, the Itoigawa–Shizuoka tectonic line, the Nojima fault, and the Koi fault (Fig. 1). The geologic setting of these faults, and the occurrence and microtexture of the fault rock samples are briefly described below.

The Tanakura shear zone is one of the major faults in Japan. The fault zone is 3 to 4 km wide, and composed of mylonite, phyllonite, cataclasite and gouge. This fault was activated mainly in the Cretaceous as a left-lateral fault and the total offset attains about 400 km (Otsuki, 1985, 1992; Otsuki and Ehiro,

Fig. 1. Locality map of the fault gouges analyzed. Solid lines denote active faults in Japan after The Research Group for Active Faults (1980).

1992). Its activation history is somewhat complicated and was reactivated lastly as a right-lateral fault in middle Miocene time. The eastern boundary fault of the shear zone in Ibaraki Prefecture strikes N15°W and is nearly vertical. Early Miocene andesite lava and breccias are in faulted contact with early Miocene conglomerate and sandstone. The conglomerate is composed of granite boulders, and the clasts are cataclastically deformed into ellipsoidal shapes. Close to the boundary fault the aspect ratio is at its largest (10:1) and the orientation of the longest axis is sub-parallel to the fault contact. The aspect ratio gradually decreases and the axial orientation rotates anticlockwise with increasing distance from the boundary fault (Fig. 2a; Otsuki, 1975). Distinct slip zones of strain localization are not developed in the conglomerate, suggesting that the cataclasis may have been due to creep faulting. The samples were collected from the cataclastically deformed granite conglomerate, and the microtexture is shown in Fig. 2b. Quartz and feldspar are crushed into very angular grains. The grain size ranges from 10 μm to the sub-millimeter scale in this photograph, but it attains several centimeters at the 1 m scale of observation.

The Itoigawa–Shizuoka tectonic line also is a major fault, and its activity has strongly controlled the development history of sedimentary basins of northeast and southwest Japan since the Miocene. It has been reactivated in the Quaternary as a thrust in both the northern and southern segments, while the middle segment was activated as a left-lateral fault.

After the 1995 Hyogo-ken Nanbu (Kobe) earthquake, the Japan Headquarters for Earthquake Research Promotion (HERP) planed to survey about 100 major active faults in order to evaluate their recent activity. The Itoigawa–Shizuoka tectonic line was included as a main target of this plan. According to the extensive study by Geological Survey of Japan and university team (Okumura et al., 1994, 1996), the recurrence time interval of seismic events is about 2000 years for the northern segment, about 1000 years for the middle segment, and about 3000 to 5000 years for the southern segment. The northern end of the southern segment is exposed in Shimotsutaki Village in Yamanashi Prefecture, where granite lies in very low angle thrust fault contact with the underlying Pleistocene conglomerate. The fault boundary is composed of a several centimeter thick gouge layer, and the granite of the hanging wall is cataclastically deformed. The mesoscopic deformation texture is rather homogeneous, but minor faults are randomly distributed. We collected several rock samples of the granite cataclasite, and a representative microtexture under the photomicroscope is shown in Fig. 3. The comminuted grains are a little smaller and more rounded than the Tanakura cataclasite. Some large grains are crushed into mosaic microstructures and the fragmented counterparts are found nearby (e.g. as indicated by the black arrow in Fig. 3a). Fig. 3b is the texture between crossed nicols, in which the trails of comminuted quartz and feldspar grains are well expressed (e.g. as indicated by the white arrow).
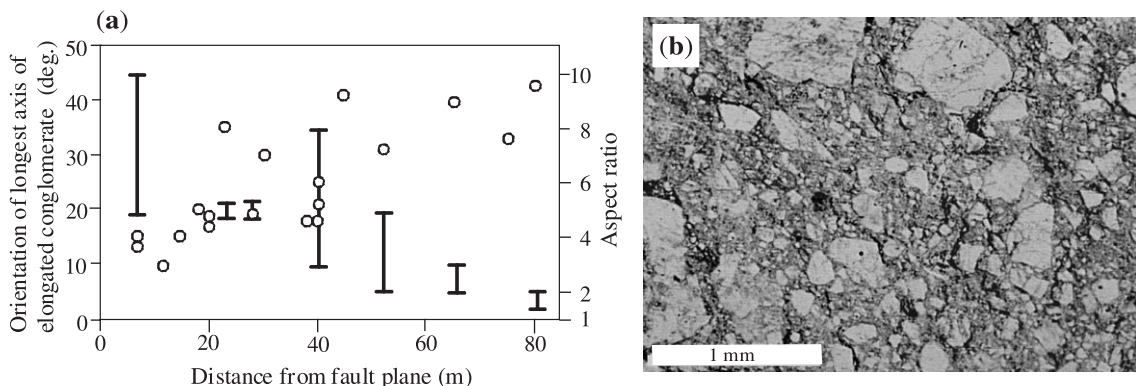

Fig. 2. (a) Aspect ratio (bar) and orientation of the longest axis (open circle: degree anticlockwise from fault plane) of elongated conglomerates adjacent to the Tanakura shear zone. (b) Optical photomicrograph showing the microtexture of the cataclastically deformed granitic conglomerate.
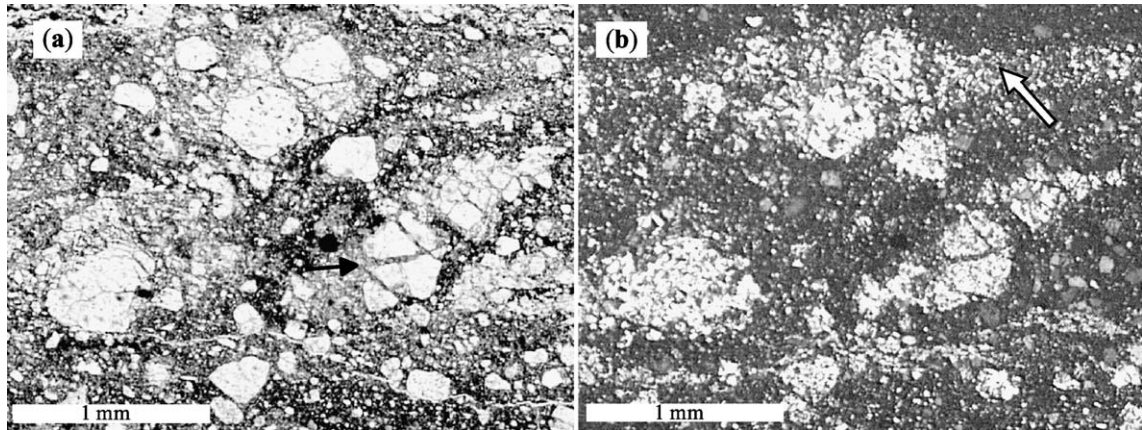
Fig. 3. Optical photomicrograph showing the microtexture of the granitic cataclasite from the Itoigawa–Shizuoka tectonic line at Shimotsutaki Village (a: through open nicol, b: between crossed nicols). Note the fragmented counterparts (arrow in a) and the trail (arrow in b) of crushed plagioclase grains.

The Koi fault is one of the NE–SW trending faults in Hiroshima Prefecture. It has not been studied in detail, but is easily identified as a geomorphologic lineament about 10 km long. The offset valleys suggest it is a right-lateral fault. Trenching was performed recently as a part of the active faults evaluation plan of HERP. According to the survey report by the Committee of Active Fault Survey for Hiroshima City Area and Fukken Survey and Designing (1996),

a fault zone of 3 to 15 cm thickness was found in the granitic basement (Fig. 4a), and the most recent seismic slip was estimated at about 1000 year B.P. by the ages of the overlying conglomerate layer that is offset and the sand layer that is not offset. The fault zone is associated with thin fault clay layers and the damaged zones on both sides. We analyzed the samples of granitic gouge from the fault core. The microtexture is shown in Fig. 4b. The sample is a little
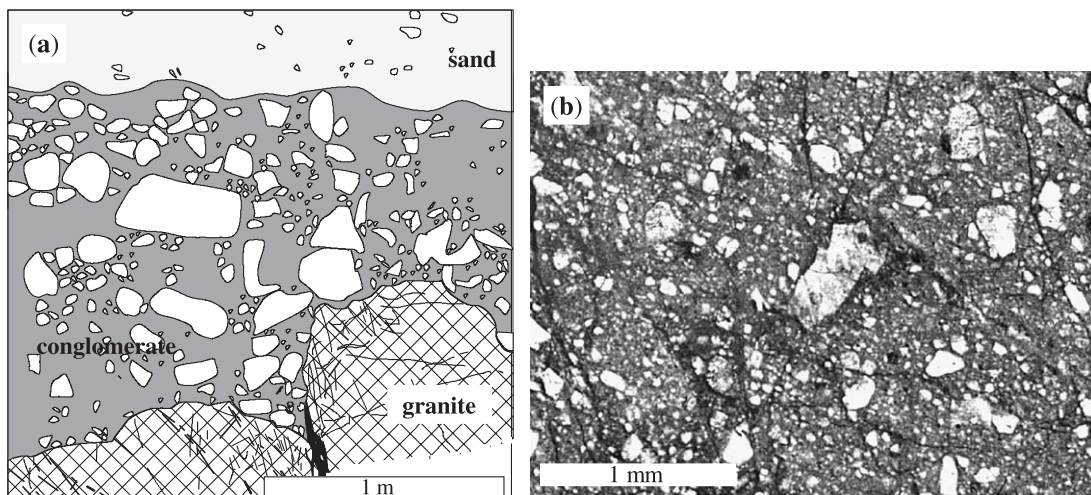

Fig. 4. (a) Fault zone of the Koi fault exposed on the trench wall (after Committee of Active Fault Survey for Hiroshima City Area and Fukken Survey an Designing, 1996). The fault zone offsets the boundary between granite basement and overlying Quaternary conglomerate, but the overlying sand layer is not affected. (b) Optical photomicrograph showing the microtexture of the gouge from the Koi fault. The microtexture is homogeneous and the grains are finer than those of the Tanakura and Shimotsutaki cataclasites.

degraded by epigenetic microcracks, but the texture is homogeneous and the grains are finer than the Tanakura and Shimotsutaki cataclasites.

The Nojima fault is a NE–SW trending right-lateral active fault along the northwestern coast of Awaji Island, Hyogo Prefecture. Its horizontal and vertical displacement rates are 0.9–1.0 and 0.4–0.5 m/ky, respectively (Mizuno et al., 1990). This fault was activated to cause the 1995 Hyogo-ken Nanbu (Kobe) earthquake (M7.2), and a 10-km-long surface rupture emerged. At the surface, the Nojima fault juxtaposes Cretaceous granite against late Pliocene fine sandstone. The fault rocks of the Nojima fault have been studied in detail in borehole samples by Ohtani et al. (2000), Tanaka et al. (2001) and Boullier et al. (2001), and for the samples from the surface outcrop by Otsuki et al. (2003). The fault plane is near vertical, and the granitic rock suffered cataclasis and hydrothermal alteration over a width of several meters. The fault core, about 20 cm thick, is sand-wiched between altered cataclastic granite and silt-stone of Osaka Group (Fig. 5a). It is composed of three kinds of fault rock; from southeast to northwest, they are highly comminuted cataclasite of granite, thinly laminated fault rock embedded in the granite cataclasite, and soft fault clay. Cataclasis of the granite is most intense in the fault core and diminishes gradually away from it, while the layers of the laminated fault rock are free from severe cataclasis. The layer of soft clay is only few cm thick, and is in contact with the laminated fault rock and granite cataclasite on the southeast side and with siltstone of the Osaka Group on the northwest side. Accommodation of the seismic slip of the 1995 Hyogo-ken Nanbu earthquake was restricted to this soft clay layer. This is evidenced by the contact relation between the laminated fault rock and the conglomeratic debris, which has smoothed over the surface rupture scarp since 1995. The plane of the contact continues smoothly into the soft fault clay layer between the
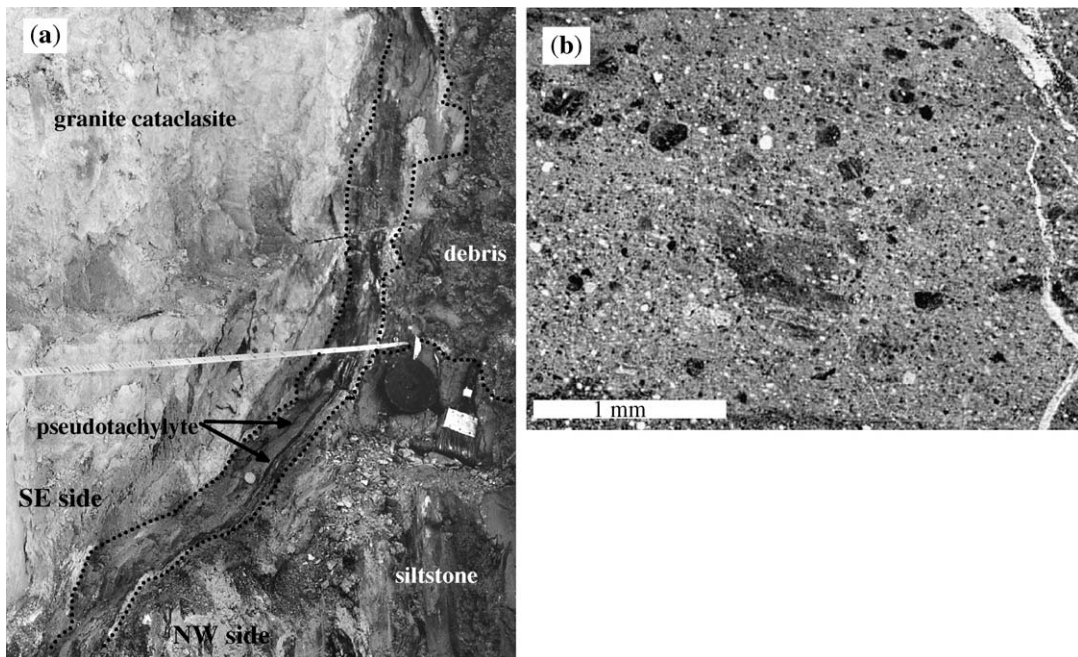

Fig. 5. (a) Nojima fault exposed on the trench wall. The fault core (between broken lines) is composed of thinly alternating layers of pseudotachylyte and solidified fine fault gouge. The left and right sides are hydrothermally altered granite cataclasite and Pliocene to Quaternary siltstone, respectively. The upper right is artificially filled debris which has smoothed over the surface rupture scarp after the 1995 Kobe earthquake. (b) Optical photomicrograph showing the microtexture of the fine fault gouge sample from the fault core of the Nojima fault. Dark and coarse grains are the fragments of old pseudotachylyte. Note that the texture is very homogeneous and the grains are very fine except the grains of pseudotachylyte fragments.

laminated fault rock and the siltstone of Osaka Group below (see the upper right of Fig. 5a).

Several layers of the laminated fault rock in the fault core extend being parallel to the fault zone, and the layer thickness ranges from a few millimeters to 1 cm. The laminated fault rock is composed of thinly alternating layers (millimeter order) of pseudotachylyte and highly cohesive very fine fault gouge derived from the granite. Otsuki et al. (2003) estimated that this laminated fault rock was formed at a depth of about 3 km by ancient seismic slip events. We deal with this fault gouge again in this paper for comparison with other fault rock samples. The microtexture of the fault gouge is shown in Fig. 5b. The fault rock texture is homogeneous and free from any localized deformational structures. The grains are the finest of all the samples from the four faults studied. Dark and relatively large grains are fragments of old pseudotachylyte. Otsuki et al. (2003) regarded this gouge to have experienced fluidization.

3. Grain size frequency of granular fault rocks

A part of the elastic energy stored in the crust is released as seismic radiation and gravity potential energy, and the remainder is dissipated through comminution and frictional heating. The proportion of the energy dissipated is an important problem concerning the seismic efficiency (Kanamori and Heaton, 2001). The size frequency of comminuted particles is an essential measure in evaluating the energy density used for comminution. Grain size distributions have been studied intensively by Sammis et al. (1986, 1987), and An and Sammis (1994) for natural faults, and by Biegel and Sammis (1989) and Marone and Scholz (1989) for experimental faults. They found that fault gouges show fractal size frequencies with fractal dimensions of about 1.6 (2-D measurements) or larger.

We present here new size frequency data for granular fault rocks from four faults (Fig. 6). The diameters of several hundreds grains were firstly measured in a fixed area of thin sections under the optical microscope at 1.25×10 magnification, and then successively in sub-areas at 4×10, 10×10 and 40×10 magnifications. The size range in which grains were measured at a magnification was set so that it overlapped widely to those at the neighboring
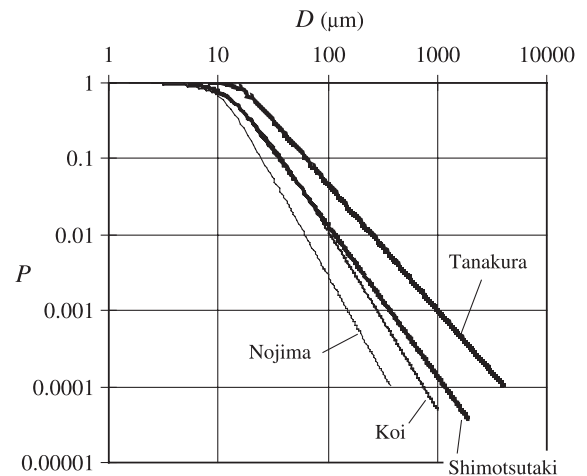

Fig. 6. Examples of size frequencies of the granular fault rocks from the Tanakura shear zone, Itoigawa–Shizuoka tectonic line at Shimotsutaki, Koi fault and Nojima fault. P denotes the cumulative probability of grains larger than diameter D. All curves have an associated cut-off at the smaller end of the grain size range.

magnifications. The size frequencies at all magnifications were combined into a grain size frequency over the wide scale of observation by multiplying an appropriate factor to the grain numbers at the adjacent larger magnification so that they become equal to those in the overlapping size range at the adjacent small magnification. This procedure was applied to several samples from each of the four faults. All data show a fractal nature with the cut-off at a small grain size, and the data plots fit well to the modified power function (Otsuki, 1998),

$$P \equiv \frac{N}{N_t} = \left[1 + \left(\frac{D}{D_c} \right)^\alpha \right]^{-\beta/\alpha} \tag{1}$$

where P is the fraction of N grains larger than diameter D among the total of grains, N_t. D_c is the characteristic diameter at the cut-off, α is a measure of the cut-off sharpness, and β is the fractal dimension.

β of the Tanakura cataclasite is the smallest of the four faults studied, ranging from 1.650 to 1.775 for five samples (mean 1.681). The mean value of D_c is 10.02 μm, being the largest of the four faults. In contrast, β of the Nojima gouge ranges from 2.192 to 2.559 for five samples (mean 2.347), being the largest, while the mean value of D_c is 7.685 μm, being the smallest among four faults. However, the resolution

limit of the optical microscope is several μm, suggesting that the D_c value of the Tanakura cataclasite is within the resolution limit, while the D_c value of the Nojima gouge is affected by the resolution limit. Therefore, the actual D_c values of the Nojima gouge may be smaller. The maximum grain size of the Tanakura cataclasite is several mm, while that of the Nojima gouge is only several hundred micrometers. Although the maximum grain size naturally depends on the scale of observation area, this cannot explain such a large difference in maximum grain size. The grain size frequencies of the Koi gouge and Shimotsutaki cataclasite show characteristics in between the Tanakura cataclasite and Nojima gouge; the average values of β and D_c are 2.090 and 11.346 μm for the Koi gouge and 2.091 and 8.108 μm for the Shimotsutaki cataclasite.

From the viewpoint of surface energy, the grain surface density is the most important statistic for evaluating the degree of comminution. We estimated the total grain boundary length, $\Sigma\pi D_i$, and the total grain area, $\Sigma\pi D_i^2/4$, by approximating all grains to be circles in a 2-D plane of observation. The plots of β against $(\Sigma\pi D_i)/(\Sigma\pi D_i^2/4)$, rearranged to $4\Sigma D_i^{-1}$, are shown in Fig. 7a. Assuming that the total grain area approximates the observation area, this figure depicts the increase of β as the density of grain boundary length increases through comminution. A similar trend has been obtained by An and Sammis (1994) for the

relation of β to the peak size in terms of mass. A more general expression of the evolutionary trend of comminution is obtained by using the alternative parameter $D_c(\Sigma D_i^{-1})$. The result is shown in Fig. 7b, where data plot close to the line

$$\beta = 2.814\, D_c \sum D_i^{-1} + 1.448, \quad R^2 = 0.9808 \quad (2)$$

The physical meaning of the parameter $D_c(\Sigma D_i^{-1})$ is the density of grain boundary length normalized by the ratio of the grain boundary length to the area of a grain with the characteristic size D_c, being equal to $4\Sigma D_i^{-1}/[\pi D_c/(\pi D_c^2/4)]$. Therefore, Eq. (2) depicts the general evolutionary trend, which holds irrespective of individual D_c values.

In powder technology, the physical significance of D_c has been understood in the relation with the concept of "the barrier at 3 μm". The origin of this barrier is mainly attributed to the size dependence of fracture strength of grains and the electric charge on the grain surfaces that binds fragmented small particles together. As a result, comminuting fragments is suppressed at this barrier, and β increases as comminution proceeds, as already discussed by An and Sammis (1994). The D_c values of our samples were not so precisely determined, but tend to decrease as comminution proceeds. Therefore, D_c is likely to be a function not only of material properties of grains, but also of the degree of comminution until D_c reaches the genuine barrier at "3 μm".
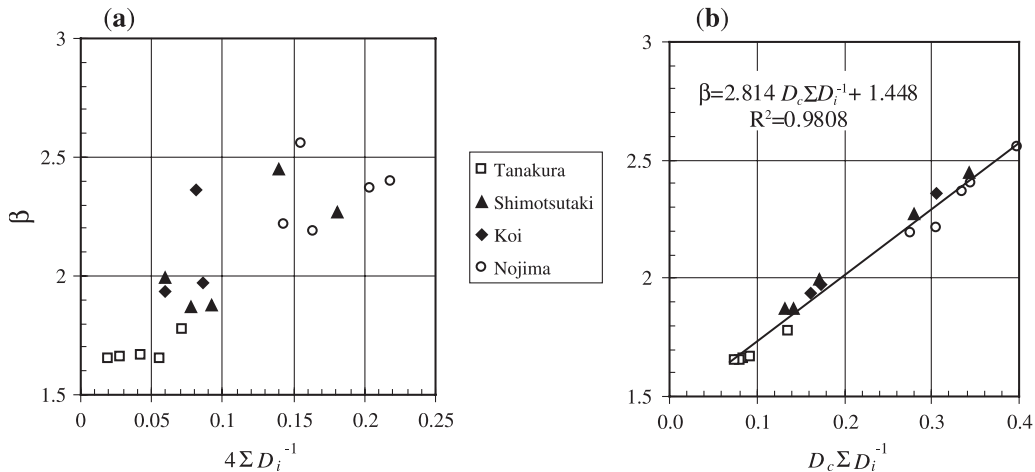

Fig. 7. Relationships between the fractal dimension β of grain size frequency and (a) the density of grain boundary length; (b) the density of grain boundary length normalized by the ratio of the grain boundary length to the area of the grain of the characteristic size D_c, for the granular fault rocks from the four faults studied. The regression line in (b) shows the general evolutionary trend of comminution.

Based on Fig. 7, the Tanakura cataclasite is interpreted to be in the earliest stage of comminution, while comminution has proceeded furthest in the Nojima gouge. The data plotted for the Shimotsutaki cataclasite and Koi gouge scatter widely on the evolutionary trend, suggesting the degree of comminution is heterogeneous, i.e. that fault slip has been localized into slip zones within the fault zone. Attention should be paid also to the fact that β values of the Tanakura cataclasite are constantly around 1.6 (corresponding to 2.6 for 3-D measurement). This value is the same as for the gouge from the Lopez fault zone, California (Sammis et al., 1987) and the gouge formed by frictional experiments (Biegel and Sammis, 1989). According to the additional data by An and Sammis (1994), the β value (3-D measurement) of gouge samples from the San Andreas fault, the San Gabriel fault and the Lopez Canyon gouge are 2.4–3.6, 2.6–2.9 and 2.4–3.0, respectively. We pay attention to the β value of 2.6, because 70% of their samples have β larger than 2.6 and even for the remaining 30% β is not smaller than 2.4. Moreover, Marone and Scholz (1989) found that the experimental comminution process started at $\beta = 2.6$ and β became significantly larger than 2.6 within the shear bands developed thereafter. Synthesizing the results by the previous authors and our data, it is highly probable that the comminution of fault rocks may start at $\beta \approx 2.6$ or just smaller value and β increases as comminution proceeds. The significance of this fact for faulting will be discussed in Section 5.

4. Fluidization of granular fault materials: its identification method and analytical results

Grain size frequency can indicate the degree of comminution. We wish here to extract the information for the fault slip behavior from the fault rock microtexture. Melosh (1979, 1996) first proposed that fault gouges could be acoustically fluidized during seismic slip to cause slip instability. Lin (1997) found very fine gouge that was injected into cracks in the fault wall rock, and regarded it as evidence of fluidization. However, granular materials like fault gouge and cataclasite can flow by frictional sliding among grains even if they are not fluidized. We here define the "fluidization" as the state in which grains fly around with a mean free path like gaseous molecules.

4.1. Outline of deformation mechanisms of granular materials

The definition of fluidization above is common in powder technology. The mechanical properties of granular materials fluidized at high shear rates have been investigated in the past by using annular shear-cell apparatus. Bagnold (1954) found two types of deformation mechanism during granular flow: a macroviscous regime and a grain-inertia regime. In the macroviscous regime stresses are transmitted by interstitial fluid friction, and are therefore dependent upon the fluid viscosity, but independent of the grain density. In the grain-inertia regime stresses are transmitted by intergranular collisions, and are therefore independent of the fluid viscosity but dependent upon the grain density. The Bagnold number B can define the transition between the two regimes,

$$B \equiv \frac{\rho_g}{\eta_f}\left[\left(\frac{\phi^*}{\phi}\right)^{1/3}-1\right]^{-1/2}d^2\dot{\gamma} \qquad (3)$$

the ratio of the inertial to the viscous forces. ρ_g and d are the specific density and diameter of spherical and equigranular solid grains in the interstitial fluid of viscosity η_f. ϕ and ϕ^* are a given volume fraction of grains and the maximum volume fraction attainable, and γ is the imposed shear strain rate.

When $B < 40$, granular flow is in the macroviscous regime, where the viscosity is nearly equal to that of the interstitial fluid. $B > 450$ defines the grain-inertia regime when, where the viscosity is significantly larger than that of the interstitial fluid. The region between these two limits is referred to as transitional. We define fluidization here as corresponding to the flow behavior in the grain-inertia regime. There is of course a third regime, the grain friction regime where grains are closely packed ($\phi \to \phi^*$, hence $B \to \infty$) and grain friction and comminution govern the macroscopic mechanical properties of granular materials. With respect to understanding the instability of seismic slip, special attention should be paid to the transition from the grain friction regime to the grain-inertia regime.

In this section, the problem is addressed of whether any diagnostic evidence of fluidization is recorded and preserved in the granular fault rock that has experienced fluidization. A newly developed analytical

method that has already been outlined by Otsuki et al. (2003) is described below in more detail.

4.2. Theoretical approach to the fragmentation of grains during fluidization

When closely packed granular materials are sheared, grains tend to be fractured by stress concentrations at the points of contact, and the probability of grains being fractured will be very high. Once the granular fault material is fluidized, grains will be comminuted by the head-on collision of flying grains and with the fault wall rock. The basic theory of fragmentation by collision is given by the Editorial Committee of Fundamentals of Granular Material Technology (1992). When two grains (radius r_1 and r_2, mass m_1 and m_2, Young's modulus Y_1 and Y_2, and Poisson's ratio v_1 and v_2) collide at a relative velocity v_c, the collision force F_c is:

$$F_c = 3.47^{1/5} \left(\frac{1 - v_1^2}{Y_1} + \frac{1 - v_2^2}{Y_2} \right)^{-2/5} \left(\frac{r_1 r_2}{r_1 + r_2} \right)^{1/5}$$
$$\times \left(\frac{m_1 m_2}{m_1 + m_2} \right)^{3/5} v_c^{6/5} \tag{4}$$

On the other hand, the tensional strength S_t of a spherical solid is related to the maximum load P_{max} in the well-known Brazilian test as,

$$P_{max} = \frac{10}{7} \pi r^2 S_t \tag{5}$$

Moreover, S_t is size-dependent as,

$$S_t = CV^{-1/n} \tag{6}$$

where V is volume and C and n are material constants. By using Eqs. (4)–(6), the critical collision velocity at which one (grain of r_1) of the two grains of same material is fragmented by head-on collision is expressed as

$$v_c = \left[0.606 \left(\frac{3}{4} \right)^{\frac{1}{n}} \pi^{\frac{2}{5} - \frac{1}{n}} C \left(\frac{1 - v}{Y} \right)^{\frac{2}{5}} \rho^{\frac{-3}{5}} r_1^{\frac{-3}{n}} r_2^{-2} (r_1 + r_2)^{\frac{1}{5}} \right.$$
$$\left. \times (r_1^3 + r_2^3)^{\frac{3}{5}} \right]^{\frac{5}{6}} \tag{7}$$

ρ in this equation denotes the specific density of the material of grain. Assuming for quartz grains

($Y = 8.71 \times 10^{10}$ Pa, $v = 0.16$, $\rho = 2.62 \times 10^3$ kgm^{-3}), v_c is about 10 m s^{-1} when $r_1 = r_2 = 1$ mm ($C = 3151$ kg m$^{2 - 3/n}$, $n = 2.57$) and 30 m s^{-1} when $r_1 = r_2 = 0.1$ mm ($C = 9748$ kgm$^{2 - 3/n}$, $n = 21.3$). The velocities assumed above are much faster than accepted seismic slip velocities (several m s^{-1} at most), and thus it can be concluded that the probability of fragmenting grains smaller than a few millimeters is virtually zero during fluidization. Conversely, grains will be fractured much more easily in the grain friction regime. The theoretical examination above suggests that the number density of fragmented counterparts may be critical in identifying whether granular fault rocks have experienced fluidization or not.

4.3. A new method to identify the fluidized granular fault rocks

During fault slip some grains will be fragmented and the fragmented counterparts will separate. This dynamic state has presumably been frozen and preserved in the fault rock. Let $N_t(r)$ be the total number of grains with radius r within an observation area of the thin section. When we define the parameter $R_f(r)$ as the fragmentation rate per one grain during unit incremental fault slip, the number of fragmented counterparts produced within the observed area during the incremental fault slip Δs is proportional to $N_t(r)R_f(r)\Delta s$. The reason for specifying the grain size is that the fracture strength is size dependent (Eq. (6)).

Fragmented grains move in various directions at various velocities, and move apart from each other as fault slip increases. They cannot be identified as fragmented counterparts any longer when they are apart beyond a critical distance d_c (see Fig. 8). Here we introduce another parameter "mean relative velocity" v_r. This is defined to be the increment of the distance between fragmented counterparts during Δs. Note that the physical dimension of v_r is not L/T but dimensionless. The mean residence "time" for the counterparts to stay within the distance d_c is d_c/v_r, and the probability at which a pair of counterpart fragments exists within the distance d_c during a fault sip event of displacement Δs after the fragmentation is proportional to $(d_c/v_r)/\Delta s$.

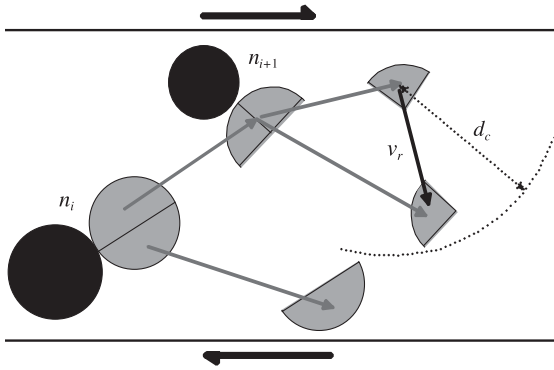Therefore, the number of grains $N_{ident}(r)$ that are identified as fragmented counterparts within a given

Fig. 8. Schematic diagram of grain collision and fragmentation process n_i, n_{i+1}... in a slip zone. Fragmented counterparts move apart from each other at a mean relative velocity v_r, and they cannot be identified as the counterparts any longer when the distance is beyond a critical value d_c.

area is proportional to $N_t(r)R_f(r)\Delta s \times d_c/v_r\Delta s$, and the detection probability $P(r)$ is expressed as,

$$P(r) \equiv \frac{N_{\text{ident}}(r)}{N_t(r)} \propto \frac{R_f(r)d_c}{v_r} \qquad (8)$$

The larger the grains, the more easily counterparts are identified. At a single scale of observation, d_c is size-dependent and may affect the P value. In the case of our study, however, this is not so, because we surveyed the grains in thin sections under an appropriate range of magnifications. Counterparts with characteristic shapes can be more easily identified, suggesting that d_c is shape-dependent, but this trivial problem was neglected in Eq. (8).

As theoretically examined already, grain fragmentation occurs very little during fluidization, i.e. it is very likely that $R_f(r)$ is very small, though it can be much larger in the grain friction regime due to stress concentrations at the grain contacts. In addition, v_r in the fluidization regime is larger than that in the grain friction regime, because in the former regime grains move with a mean free path, while they are closely packed in the latter regime. As a result, very small $P(r)$ is expected for fluidized granular fault materials, whereas it will be much larger for non-fluidized ones.

4.4. Analytical results for P(r)

We measured $P(r)$ for the Nojima, Koi, Shimotsutaki and Tanakura fault rocks (Fig. 9). The P value of

the Tanakura cataclasite is the largest of the four samples. It attains 50% for the diameter ($2r$) of around 1 mm and becomes smaller to 11% as the diameter decreases to 20 μm. This size dependency of P mainly reflects the size dependency of S_t (and hence R_f). The Shimotsutaki cataclasite also shows high P values, and size dependency. In contrast to these two samples, it is noteworthy that the P values of the Koi and Nojima gouges are very small. The P values of the Koi gouge are smaller than several percent over the full size range, although a slight size dependency is recognizable. The P values of the Nojima gouge are nearly zero over the whole range of grain size (average: 0.2%). Attention should be paid to the P value gap between two sample groups, first group of the Tanakura and Shimotsutaki cataclasites and the second group of the Nojima and Koi gouges. From the contexts in the preceding subsections, it is reasonable to conclude that the former group can be correlated to the products in the grain friction regime, and the latter to those of fluidization.

This conclusion is not inconsistent with the textural characteristics described in Section 2. Many
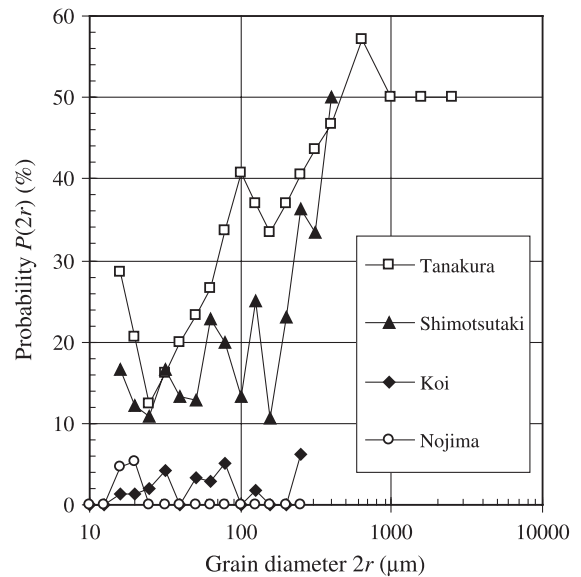

Fig. 9. Detection probability P of fragmented counterparts as a function of grain diameter $2r$ for the Tanakura cataclasite, Shimotsutaki cataclasite, Koi gouge and Nojima gouge. The smaller the grains, the smaller the P value, reflecting the size dependency of grain strength. Note that the P values of Nojima and Koi gouges are much smaller than those of the Tanakura and Shimotsutaki cataclasites.

stick–slip experiments (e.g. Byerlee, 1978; Moore et al., 1989) showed that seismic slips tend to localize in the main displacement shears and the Riedel shears. Therefore, the Tanakura cataclasite, which is not associated with distinct zones of deformation localization, is likely to have been deformed by creep faulting in which comminution proceeds in the grain friction regime. In contrast, seismic slips along the Nojima fault have repeated within the fault core about 20 cm wide, and the slip of each seismic event has been localized to a few mm thick slip zone where fault gouge was fluidized and melted by frictional heating (Otsuki et al., 2003). The microtexture within the gouge layer corresponding to each seismic event also is very homogeneous (see Fig. 5b) and lacks any structure of slip localization like Riedel shear. However, the origin of the homogeneous texture of the Nojima gouge is very different from that of the Tanakura cataclasite; the former is attributed to the homogenization by fluidization resulting from extreme slip localization, while the latter is a direct result of non-localized deformation. The microtexture of the Koi gouge also is homogeneous and similar to the Nojima gouge. Microtexture of the Shimotsutaki cataclasite is different from those of the Nojima and Koi gouges. As shown in Fig. 3, the fragmented counterparts are frequently found near each other. Moreover, the trails of crushed feldspar and quartz grains are developed. Such microstructures may be neither formed nor preserved in the fluidization regime.

5. Discussions and implications of comminution and fluidization to fault slip behavior

We will discuss below the implications of comminution and fluidization of granular materials to faulting behavior and on the plausible mechanisms of fluidization.

5.1. Fractal dimension 2.6 of grain size frequency; what does it mean?

We have pointed out in Section 3 that comminution of fault rocks may start at fractal dimension β of grain size frequency close to 2.6 (3-D measurement), and it increases as comminution proceeds. Sammis et

al. (1987) gave an intuitive explanation for the meaning of $\beta = 2.6$ that the probability of same size grains neighboring each other becomes smallest at this value. Here we will discuss this problem from a simpler viewpoint.

We investigated the relationship between β and ϕ^* (maximum volume fraction of grains attainable) for granular materials. Spherical glass beads of five different diameters (0.5, 1.0, 3.0, 6.0 and 12 mm) were prepared, and mixed them at various volume fractions to make quasi-fractal granular materials with various fractal dimensions. Their ϕ^* values were estimated from the volume of water immersed, bearing in mind that ϕ^* changes a little depending on packing state. We measured ϕ^* for loose packing as soon as the granular material was placed into the container, and ϕ^* for close packing in which the former was shaken thereafter. As shown in Fig. 10, ϕ^* values show maximum at β around 2.5 for both cases. In order to check the result of these tentative experiments, we performed numerical simulations for randomly packed spherical granular materials with ideally fractal size frequency within a limited size
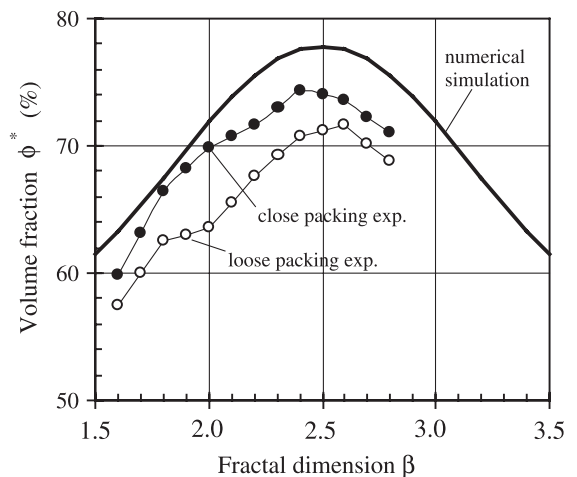

Fig. 10. Relationships between the fractal dimension β (3-dimensional measurement) of grain size frequency and the maximum volume fraction ϕ^* attainable. Open and solid circles are the results of random loose and close packing experiments for spherical glass beads of quasi-fractal size frequency, respectively. Solid line denotes the result of numerical simulation for random close packing of spherical grains of ideally fractal size frequency within a limited size range. The simulation code made by Suzuki et al. (1999) was used. ϕ^* is maximum at β around 2.5 for all cases.

range by using the computer code made by Suzuki et al. (1999). The result shown in Fig. 10 is very consistent with the results from the laboratory experiments although the ϕ^* values are larger due to the effect of ideally fractal size frequency.

From these findings, a new explanation for the special β value about 2.6 observed for natural fault rocks is provided as follows. When the granular material with fractal size frequency is randomly packed, ϕ^* becomes maximum at β very close to 2.5 (3-D measurement). This packing state minimizes the interstices, a given grain can be supported by largest number of neighboring grains possible, and hence the granular material in this state is strongest. The results in Fig. 10 show that ϕ^* values are maximum at β very close to 2.5 and decrease monotonously as β increases. Given that comminution of natural fault rocks starts at a β of about 2.6 and β increases as comminution proceeds, we conclude that comminution itself is a kind of slip weakening mechanism.

5.2. Frictional property of fluidized granular fault materials

Bagnold (1954) found very important empirical relationships among shear stress τ, normal stress σ_n and the friction coefficient μ_s of the granular materials in the grain-inertia regime.

$$\tau \propto \sigma_n \propto \rho_g \left[\left(\frac{\phi^*}{\phi} \right)^{1/3} - 1 \right]^{-2} (d\dot{\gamma})^2, \quad \mu_s \equiv 0.32 \quad (9)$$

Here we must note that σ_n is not the imposed stress but the generated stress by the collision of flying grains to the parallel solid walls of the shear-cell apparatus. The relationships of Eq. (9) were fundamentally supported experimentally (Savage and Sayed, 1984; Hanes and Inman, 1985) and theoretically (Savage and Jeffrey, 1981; Jenkins and Savage, 1983) thereafter.

Eq. (9) does not express explicitly the effect of interstitial fluid viscosity η_f, but the effective viscosity η_s of suspended granular materials can be written as $\eta_s \propto d^2[(\phi^*/\phi)^{1/3} - 1]^{-2} \dot{\gamma}$ as a function of d, $\dot{\gamma}$ and ϕ. Based on many experimental data at constant $\dot{\gamma}$, several empirical equations of η_s that include η_f explicitly as a parameter have been proposed by powder technolo-

gists (Thomas, 1965; Krieger, 1972; Barnea and Mizrahi, 1973; Metzner, 1985). The difference of the equations is partly due to the differences in range of parameters experimented used in the experiments (Metzner, 1985). Among the empirical equations,

$$\eta_s = \eta_f \left(1 - \frac{\phi}{\phi^*} \right)^{-K\phi^*}, \quad K = 3.12, \quad \phi^* = 0.647 \quad (10)$$

by Krieger (1972) appears to be most appropriate. $K\phi^* = 2.018$, and $(\phi^*/\phi) - 1$ is very close to $1 - (\phi/\phi^*)$, so that the essential difference between Eqs. (9) and (10) is the difference in power of ϕ/ϕ^*. The 1/3 power in Eq. (9) was derived rather from the simple consideration on the ideal packing geometry than the experimental result (Bagnold, 1954), and the effect of ϕ is greater in Eq. (10) than in Eq. (9). One reason why these two types of equations have been used may be the difficulty in obtaining accurate experimental data at ϕ very close to ϕ^*, as discussed below.

In order to overview the dependency of η_s on the wide ranges of $\dot{\gamma}$ and ϕ/ϕ^*, we synthesized the experimental data of several authors (Metzner and Whitlock (1958); Metzner, 1985; Hoffman, 1972; Nicodemo et al., 1974; Barnes, 1989; Frith et al., 1996) into Fig. 11. When ϕ/ϕ^* is small, the relative viscosity η_s/η_f is kept small (the order of 10) over the whole range of $\dot{\gamma}$ (10^{-1} to 10^3/s). It gradually increases as ϕ/ϕ^* increases. The former and latter regions correspond to the macro-viscous regime and the grain-inertia regime respectively of Bagnold (1954). In the region of ϕ/ϕ^* larger than about 0.77, η_s/η_f increases dramatically by shear thickening and jumps more than two orders of magnitude. As ϕ/ϕ^* approaches 1, η_s/η_f fluctuates in a complex manner with large amplitudes, although this is not fully depicted in Fig. 11. This was attributed to the instantaneously alternating changes in ordered/disordered arrangement of grains (Hoffman, 1972) and clustering/de-clustering of grains (Barnes, 1989; Frith et al., 1996).

The most important point from this figure is that the determinative cause of the fluidization is the slight decrease in ϕ/ϕ^* from 1, and that once fluidized, the frictional strength of the fault materials decreases dramatically. When we use the data by Hanes and Inman (1985) and Eq. (9), τ is only 318 Pa when $\rho_g = 2400$ kg/m³, $d = 100$ μm, $\dot{\gamma} = 1000$/s, and $\phi/\phi^* = 0.984$ for example. Therefore we conclude that
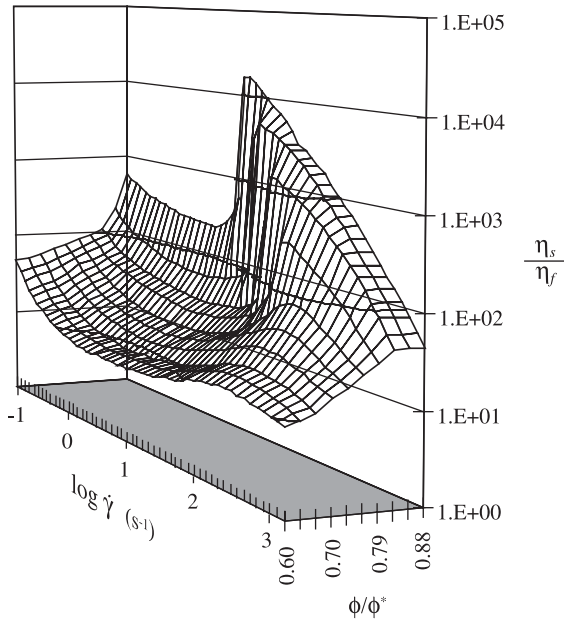
Fig. 11. Viscosity η_s of spherical equigranular materials normalized by the viscosity η_f of interstitial fluids as a function of shear strain rate $\dot{\gamma}$ and the volume fraction ϕ of grains normalized by the maximum volume fraction ϕ^* of grains attainable. Obtained from a synthesis of the experimental results of Metzner (1985), Metzner and Whitlock (1958), Hoffman (1972), Nicodemo et al. (1974), Barnes (1989) and Frith et al. (1996).

nearly complete stress drop occurs simultaneously with the fluidization of granular fault materials.

5.3. Examination of some plausible causes of fluidization in nature

As known already, frictional resistance decreases dramatically during the phase transition from the grain friction regime to fluidization, and this phenomenon is very important for seismic slip behavior. B in Eq. (3) was originally defined in the macroviscous and grain-inertia regimes, but the grain size reduction may potentially promote this phase transition. This may be one of the reasons why the granular fault rocks identified as having been fluidized in Section 4 show smaller grain size than the non-fluidized ones.

Eqs. (3), (9) and (10) tell us that ϕ/ϕ^* is the most deterministic parameter of the phase transition, because, as known already, it is caused by very slight decreases in ϕ/ϕ^* from 1. We must use these equations carefully, because they were established

fundamentally for spherical equigranular materials. The ϕ^* value of spherical equigranular grains is 0.68 (Kataoka et al., 1978; Kitano et al., 1981) or 0.647 (Frith et al., 1996), interestingly close to 0.645 in the case of random close packing (Onoda and Liniger, 1990). On the other hand, we already know that the size frequency of granular fault materials shows a fractal nature, and we have presented the experimental ϕ^* values in Fig. 10 as a function of fractal dimension β. Whether Eqs. (3), (9) and (10) hold for fractal granular materials or not may be determined from the experimental data of Chong et al. (1971). They performed experiments on bimodal suspensions (volume fraction of small grains was kept constant at 25% and size ratio was changed), showing that their experimental data fitted well to the $\eta_s = \eta_f[1 - 0.75\phi/(\phi^* - 0.25)]^{-2}$. Therefore, these equations seem likely to hold fundamentally if only ϕ^* value of fractal granular materials is adopted and an appropriate pre-ϕ/ϕ^* constant is assumed.

One way to decrease ϕ/ϕ^* is by increasing ϕ^*. However, as presented in Fig. 10, ϕ^* decreases as comminution proceeds, and a decrease in ϕ/ϕ^* can never be realized by comminution under constrained conditions. Another way to decrease ϕ/ϕ^* is to decrease ϕ, which can only be achieved under unconstrained conditions, most likely by widening of the gap between fault wall rocks which allow the grains to move with a mean free path. On this point, the mechanism of acoustic fluidization of fault gouge proposed by Melosh (1979, 1996) is noteworthy. According to him, a part of earthquake energy is released as high-frequency acoustic waves that scatter off and shake the granular fault materials leading to the build-up of a local acoustic pressure. When this pressure becomes of the order of the overburden lithostatic pressure, the granular material becomes essentially free to slip without much residual friction. However, Sornette and Sornette (2000) pointed out some serious misunderstandings in his theory that stem from a confusion in the definition of dissipation and scattering lengths.

The thermal pressurization (e.g. Sibson, 1977; Lachenbruch, 1980; Mase and Smith, 1987) will work inevitably during seismic slips. According to Mase and Smith (1987), when permeability and compressibility of porous media are smaller than 10^{-18} m^2 and 10^{-9} Pa^{-1}, respectively, it works most effectively

and the fluid pressure can approach lithostatic pressure and shear strength approaches zero. The gap between fault wall rocks could be widened by the thermally pressurized interstitial fluid, but this is unlikely if the fluid pressure never exceeds the normal stress on the wall rock.

5.4. Normal interface vibration: a most plausible cause of fluidization in nature

We have known already that the fluidization of granular fault materials needs the coseismic widening of the gap between fault wall rocks. The normal interface vibration by Brune et al. (1993) appears to be most appropriate for it. Based on engineering literatures (e.g. Schallamach, 1971) and their own frictional experiments between foam rubber blocks, they concluded that stick−slip shear motion is associated with various degrees of fault separation leading to reduced dynamic fault friction. According to the recent stick−slip experiment by Bouissou et al. (1998) using polymethylmethacrylate sliders, the fault separation increases as the applied normal stress and the surface roughness increase, and they interpreted the mechanism of self-healing pulse by Heaton (1990) as a result of interlocking of asperities when sliding surfaces come back into contact. Evidence of coseismic fault plane separation is very rare, but Brune et al. (1993) cited a personal communication from R. Sharp that the 1976 Guatemala earthquake (M_s 7.5) had a minimum of 3−4 cm of motion perpendicular to the trace of the fault, at least locally.

We found two lines of indirect evidence of fault plane separation during the 1995 Hyogo-ken Nanbu earthquake. First one is the crosscut timing relation of fault striations formed during one seismic slip event on one seismic fault plane. Otsuki et al. (1997) and Spudich et al. (1998) described the curved striations formed during the earthquake. The slip vector at the initial slip phase has the rake of several tens of degrees, but became nearly horizontal at the final stage. It was typically observed at Hirabayashi Village that high angle striations of the initial phase of slip were crosscut by low angle striations of the final phase. According to Otsuki et al. (1997), the crosscutting relation at this locality is due to the effect of the ground surface topography. However, a similar crosscutting relation was observed at Ogura Village (about 2 km southwest

from Hirabayashi Village) where the seismic fault scarp appeared on the flat ground surface. The fault scarp was dried up to collapse readily, but fortunately the crosscutting relation was well preserved on the thin blocks fallen down from the fault scarp (Fig. 12), and their original positions could be easily known from their characteristic shapes. Nearly horizontal striations of the final slip phase have overprinted directly the striations of the initial phase with the rake of about 40° NE, with striations of an intermediate slip phase lacking. This suggests that the fault plane was opened instantaneously during the intermediate slip phase.

After the 1995 Hyogo-ken Nanbu earthquake, a trench excavation study was performed at the same locality of Fig. 12. According to our observations of the trench walls, coarse sand grains and round pebbles were sandwiched between the fault wall rocks (Fig. 13). It is very likely that these grains were derived from ground surface, because they are highly oxidized to a deep brown color and could be easily distinguished from the sandstone and siltstone of the fault walls. The sandwiched layer is thick in the upper part and was recognized continuously from the ground surface to a depth of 1.5−2 m. A similar phenomenon was also observed in the trench excavated at Hirabayashi Village. The fault planes were of course
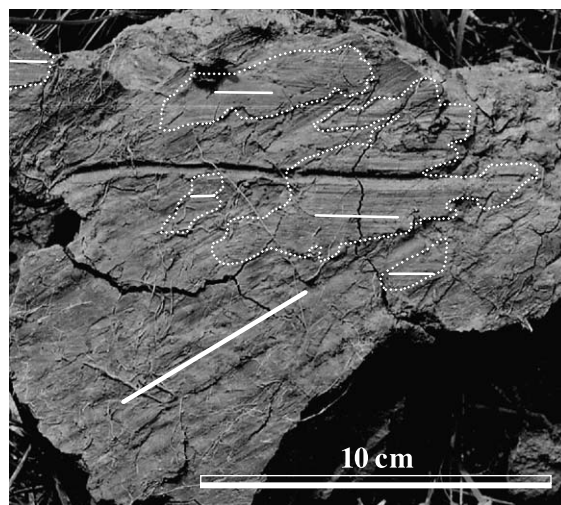

Fig. 12. Crosscutting striations formed on the fault surface of the Nojima seismic fault during the 1995 Hyogo-ken Nanbu earthquake. The high angle striations of the early slip phase are overprinted by the horizontal striations of the later slip phase. Note that striations of the intermediate slip phase were not recorded.
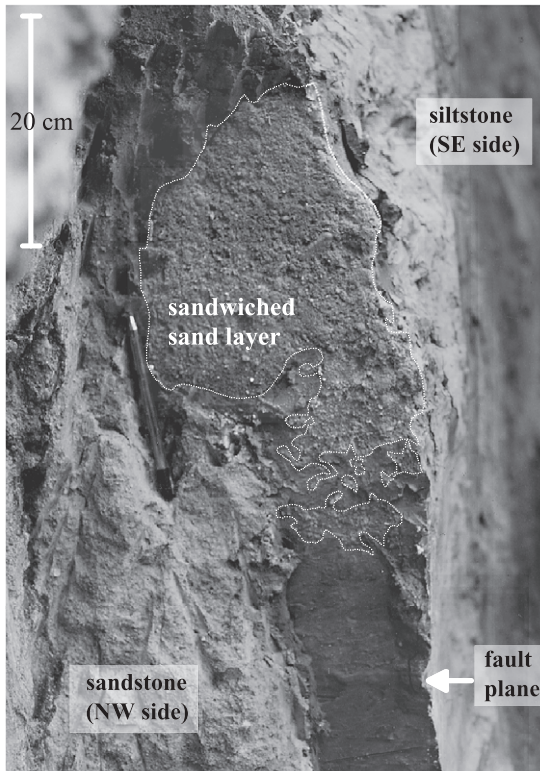
Fig. 13. A thin layer sandwiched between the sandstone fault wall of northwest side and the siltstone fault wall of southeast side of the Nojima seismic fault at Ogura Village, Awaji Island. The layer is composed of strongly oxidized exotic coarse sand grains and pebbles that fell down from the ground surface probably during the 1995 Hyogo-ken Nanbu earthquake.

already closed during the trench excavation surveys. Therefore, it is highly probable that the fault plane opening was instantaneous, probably during the seismic slip event. From the depth that the grains reached, the time intervals during which the fault plane was kept open are roughly calculated to be about 0.5 to 0.6 s at most.

The two kinds of phenomena described above were observed at a limited number of localities at the surface. Therefore, we cannot preclude the possibility that the fault plane separation suggested may be due to irregular topography of the fault plane or a special effect of the free boundary ground surface, but they appear to support the normal interface vibration of Brune et al. (1993). If fault planes are opened by this mechanism, ϕ will inevitably decrease and granular fault materials will become fluidized.

6. Conclusions

(a) The cumulative size frequency of granular fault rocks has a fractal nature. Comminution of fault rocks is likely to start at a fractal dimension β close to 2.5 (3-D measurement). When β is 2.5, the interstices of fractal granular materials are minimized and a given grain can be supported by the maximum number of grains possible. Therefore, the fractal granular material is strongest during initial comminution. As comminution proceeds, β increases, and the interstices also increase steadily. Therefore, comminution itself is a slip weakening mechanism.

(b) We have developed a method to distinguish the granular fault rocks that have experienced fluidization from non-fluidized ones, in which the detection probability of fragmented counterparts is a key parameter. This method was successfully applied to several fault rock samples. This method can be a useful tool for paleoseismologists to identify whether active faults have moved by seismic faulting or creep faulting.

(c) The most probable cause of fluidization of granular fault materials is the normal interface vibration by Brune et al. (1993). Our new field evidence for fluidization of granular fault rocks and coseismic fault plane opening support that the normal interface vibration may work in nature.

(d) Once granular fault materials are fluidized, slip zones become nearly frictionless, and sudden and nearly complete stress drop will occur, even if thermal pressurization does not work effectively and even before it reaches its extreme state.

References

An, L., Sammis, C.G., 1994. Particle size distribution of cataclastic fault materials from southern California: a 3-D study. PAGEOPH 143, 203–227.

Bagnold, R.A., 1954. Experiments on a gravity-free dispersion of large solid spheres in a Newtonian fluid under shear. Proc. R. Soc. London, Ser. A 225, 49–63.

Barnea, E., Mizrahi, J., 1973. A generalized approach to the fluid dynamics of particulate systems. Chem. Eng. Sci. 5, 171–189.

Barnes, H.A., 1989. Shear-thickening ("dilatancy") in suspensions of non-aggregating solid particles dispersed in Newtonian liquids. J. Rheol. 33, 329–366.

Biegel, R.L., Sammis, C.G., 1989. The frictional properties of a simulated gouge having a fractal particle distribution. J. Struct. Geol. 11, 827–846.

Bouissou, S., Petit, J.P., Barquins, M., 1998. Experimental evidence of contact loss during stick–slip: possible implications for seismic behavior. Tectonophysics 295, 341–350.

Boullier, A.M., Ohtani, T., Fujimoto, K., Ito, H., Dubois, M., 2001. Fluid inclusions in pseudotachylytes from the Nojima fault, Japan. J. Geophys. Res. 106, 21965–21977.

Brune, J.N., Brown, S., Johnson, P.A., 1993. Rupture mechanism and interface separation in foam rubber models of earthquakes: a possible solution to heat flow paradox and the paradox of large overthrusts. Tectonophysics 218, 59–67.

Byerlee, J.D., 1978. Friction of rocks. PAGEOPH 116, 615–626.

Chong, J.S., Christiansen, E.B., Baer, A.D., 1971. Rheology of concentrated suspensions. J. Appl. Polym. Sci. 15, 2007–2021.

Committee of Active Fault Survey for Hiroshima City Area and Fukken Survey and Designing, 1996. Survey Report for Koi Fault and Other Two Active Faults. 137 pp.

Editorial Committee of Fundamentals of Granular Material Technology, 1992. Fundamentals of Granular Material Technology. Nikkan Kogyo Shinnbun-sha, Tokyo. 411 pp. (in Japanese).

Frith, W., d'Haene, J., Buscall, P.R., Mewis, J., 1996. Shear thickening in model suspensions of sterically stabilized particles. J. Rheol. 40, 531–548.

Hanes, D.M., Inman, D.L., 1985. Observations of rapidly flowing granular-fluid materials. J. Fluid Mech. 150, 357–380.

Heaton, T.H., 1990. Evidence for and implications of self-healing pulses of slip in earthquake rupture. Phys. Earth Planet. Inter. 64, 1–20.

Hoffman, R.L., 1972. Discontinuous and dilatant viscosity behavior in concentrated suspensions, I. Observation of a flow instability. Trans. Soc. Rheol. 16, 155–173.

Jenkins, J.T., Savage, S.B., 1983. A theory for the rapid flow of identical, smooth, nearly elastic, spherical particles. J. Fluid Mech. 130, 187–202.

Kanamori, H., Heaton, T., 2000. Microscopic and macroscopic physics of earthquakes. In: Rundle, J., Turcotte, D., Klein, W. (Eds.), GeoComplexity and the Physics of Earthquakes. Geophys. Monogr. Ser., vol. 120. AGU, Washington, DC, pp. 147–183.

Kataoka, T., Kitano, T., Sasahara, M., Nishijima, K., 1978. Viscosity of particle filled polymer melts. Rheol. Acta 17, 149–155.

Kitano, T., Kataoka, T., Shirota, T., 1981. An empirical equation of the relative viscosity of polymer melts filled with various inorganic fillers. Rheol. Acta 20, 207–209.

Krieger, I.M., 1972. Rheology of monodisperse lattice. Adv. Colloid Interface Sci. 46, 491–506.

Lachenbruch, A.H., 1980. Frictional heating, fluid pressure, and the resistance to fault motion. J. Geophys. Res. 85, 6097–6112.

Lin, A., 1997. Fluidization and rapid injection of crushed fine-grained materials in fault zones during episodes of seismic faulting. In: Zheng, et al., (Eds.), Proc. 30th Int'l. Congr., vol. 14. VSP, Tokyo, pp. 27–40.

Marone, C., Scholz, C., 1989. Particle-size distribution and microstructures within simulated fault gouge. J. Geophys. Res. 11, 799–814.

Mase, C.W., Smith, L., 1987. Effect of frictional heating on the thermal, hydrologic, and mechanical response of a fault. J. Geophy. Res. 92, 6249–6272.

Melosh, H.J., 1979. Acoustic fluidization: a new geological process? J. Geophys. Res. 84, 7513–7520.

Melosh, H.J., 1996. Dynamic weakening of faults by acoustic fluidization. Nature 379, 601–606.

Metzner, A.B., 1985. Rheology of suspensions in polymeric liquids. J. Rheol. 29, 739–775.

Metzner, A.B., Whitlock, M., 1958. Flow behavior of concentrated (dilatant) suspension. Trans. Soc. Rheol. 11, 239–254.

Mizuno, K., Hattori, H., Sangawa, A., Takahashi, Y., 1990. Geology of the Akashi district, quadrangle-series, scale 1:50,000. Geol. Surv. Jpn., Tsukuba, Japan, 90 (in Japanese with English abstract).

Moore, D.E., Summers, R., Byerlee, J.D., 1989. Sliding behavior and deformation textures of heated illite gouge. J. Struct. Geol. 11, 329–342.

Nicodemo, L., Nicolais, L., Landel, R.F., 1974. Shear rate dependent viscosity of suspensions in Newtonian and non-Newtonian liquids. Chem. Eng. Sci. 29, 729–735.

Ohtani, T., Fujimoto, K., Ito, H., Tanaka, H., Tomida, N., Higuchi, T., 2000. Fault rocks and past to recent fluid characteristics from the borehole survey of the Nojima fault ruptured in the 1995 Kobe earthquake, southwest Japan. J. Geophys. Res. 105, 16161–16171.

Okumura, K., Shimokawa, K., Yamazaki, H., Tsukuda, E., 1994. Recent surface faulting events along the middle section of the Itoigawa–Shizuoka tectonic line. Zisin 46, 425–438 (in Japanese).

Okumura, K., Imura, R., Imaizumi, T., Sawa, H., Togo, M., 1996. Paleoseismological study of the Itoigawa–Shizuoka tectonic line active fault system. Study Rep. Geol. Surv. Jpn. 259, 89–94 (in Japanese).

Onoda, G.Y., Liniger, E.G., 1990. Random loose packing of uniform spheres and the dilatancy onset. Phys. Rev. Lett. 64, 2727–2731.

Otsuki, K., 1975. Geology of Tanakura shear zone and adjacent area. Tohoku Univ. Inst., Geol. Pal. Contr. 76, 1–71 (in Japanese).

Otsuki, K., 1985. Plate tectonics of eastern Eurasia in the light of fault systems. Tohoku Univ. Sci. Rep. (Geology) 55, 141–251 (2nd ser.).

Otsuki, K., 1992. Oblique subduction, collision of micro-continents

and subduction of oceanic ridge: their implications on the Cretaceous tectonics of Japan. Isl. Arc 1, 51–63.

Otsuki, K., 1998. An empirical evolution law of fractal size frequency of fault population and its similarity law. Geophys. Res. Lett. 25, 671–674.

Otsuki, K., Ehiro, M., 1992. Cretaceous left-lateral faulting in Northeast Japan and its bearing on the origin of geologic structure of Japan. J. Geol. Soc. Jpn. 98, 1097–1112 (in Japanese).

Otsuki, K., Minagawa, J., Aono, M., Ohtake, M., 1997. On the curved striations of Nojima seismic fault engraved at the 1995 Hyogoken–Nambu earthquake, Japan. Zisin 49, 451–460.

Otsuki, K., Monzawa, N., Nagase, T., 2003. Fluidization and melting of fault gouge during seismic slip: identification in the Nojima fault zone and implications for focal earthquake mechanism. J. Geophys. Res. (in press).

Sammis, C.G., Osborne, R.H., Anderson, J.L., Banerdt, M., White, P., 1986. Self-similar cataclasis in formation of fault gouge. PAGEOPH 124, 53–78.

Sammis, C., King, G., Biegel, R., 1987. The kinetics of gouge deformation. PAGEOPH 125, 777–812.

Savage, S.B., Jeffrey, D.J., 1981. The stress tensor in a granular flow at high shear rates. J. Fluid Mech. 110, 255–272.

Savage, S.B., Sayed, M., 1984. Stresses developed by dry cohesionless granular materials sheared in an annular shear cell. J. Fluid Mech. 142, 391–430.

Schallamach, A., 1971. How does rubber slide? Wear 17, 301–312.

Sibson, R.H., 1977. Kinetic shear resistance, fluid pressure, and relation efficiency during seismic faulting. PAGEOPH 115, 387–400.

Sornette, D., Sornette, A., 2000. Acoustic fluidization for earthquakes? Bull. Seismol. Soc. Am. 90, 781–785.

Spudich, P., Guatteri, M., Otsuki, K., Minagawa, J., 1998. Use of fault striations and dislocation models to infer tectonic shear stress during the 1995 Hyogo-ken Nanbu (Kobe) earthquake. Bull. Seismol. Soc. Am. 88, 413–427.

Suzuki, M., Kada, H., Hirota, M., 1999. Effect of size distribution on relation between coordination number and void fraction of spheres in randomly packed bed. Adv. Powder Technol. 10, 353–365.

Tanaka, H., Fujimoto, K., Ohtani, T., Ito, H., 2001. Structural and chemical characterization of shear zones in the freshly activated Nojima fault, Awaji Island, southwest Japan. J. Geophys. Res. 106, 8786–8810.

The Research Group for Active Faults, 1980. Active Faults in Japan, Sheet Maps and Inventories. University of Tokyo Press, Tokyo. 363 pp.

Thomas, D.G., 1965. Transport characteristics of suspension: VIII. A note on the viscosity of Newtonian suspensions of uniform spherical particles. J. Colloid Sci. 20, 267–277.